



Observing subcanopy CO₂ advection

Ralf M. Staebler*, David R. Fitzjarrald

Atmospheric Sciences Research Center, University at Albany, SUNY, 251 Fuller Road, Albany, NY 12203, USA

Received 7 April 2003; received in revised form 29 September 2003; accepted 29 September 2003

Abstract

Underestimation of nocturnal CO₂ respiration under calm conditions remains an unsolved problem at many forest flux stations. In this paper, the hypothesis is tested that horizontal mean transport, not previously measured, may account for the missing CO₂. A systematic methodology was developed that comprises characterizing the subcanopy motions, determining the appropriate size of the subcanopy network required to make the measurements, developing a method of integrating the measurements in the vertical, and determining the required averaging time. Measurements were performed at the Harvard Forest (Petersham, MA), over 4 years. The appropriate size of the network of wind and CO₂ sensors was shown to be on the order of 100 m, ensuring that sensors were generally observing coherent processes on this scale or larger and thus displayed some correlation. Horizontal transport of CO₂ at Harvard Forest was found to be restricted to the bottom ~10 m of the forest. The fraction of the negative buoyancy force in the sum of dynamic driving forces described nights with missing flux problems (“deficit nights”) significantly better than the commonly used friction velocity criterion. Including the measured horizontal transport terms did not on average fully account for the observed difference in NEE of $1.2 \pm 0.3 \mu\text{mol m}^{-2} \text{s}^{-1}$ between deficit and non-deficit nights, but decreased the difference to $0.7 \pm 0.5 \mu\text{mol m}^{-2} \text{s}^{-1}$. Horizontal transport did account for the difference, to within measurement error, during summer months, but not during spring or fall. Crown Copyright © 2003 Published by Elsevier B.V. All rights reserved.

Keywords: Carbon dioxide flux; Forest carbon budget; Horizontal advection

1. Introduction

It is generally accepted that the current methods of estimating net ecosystem exchange (NEE = turbulent flux plus storage) underestimate nocturnal respiration of CO₂ from forests on calm nights (Wofsy et al., 1993; Black et al., 1996; Goulden et al., 1996; Lavigne et al., 1997). In most forests, ecologically reasonable NEE estimates are obtained at higher levels of turbulence, but during conditions of low winds, and associated low turbulence (low friction velocity, u_*),

eddy fluxes are significantly smaller although there are no ecological reasons to expect that respiration should be inhibited. In these conditions, respired CO₂ must be transported away from its source by some other mechanism, undetected by standard techniques. Potential candidates for these mechanisms include the vertical and horizontal advection terms generally not considered under assumptions of horizontal homogeneity. Quantification of nocturnal, respiratory CO₂ fluxes is a major issue. For example, whether the Amazon rain forest is considered a sink or source of atmospheric carbon may depend on accurate estimates of CO₂ fluxes at night (Miller et al., 2003).

In this paper, we test the hypothesis that nocturnal CO₂ fluxes that are missed by EC plus storage can be accounted for by including advection terms in the

* Corresponding author. Present address: Air Quality Research Branch, Meteorological Service of Canada, 4905 Dufferin Street, Downsview, Ont., Canada M3H 5T4. Tel.: +1-416-739-5730; fax: +1-416-739-5708.

E-mail address: ralf.staebler@ec.gc.ca (R.M. Staebler).

transport equation that are usually neglected. Data were collected at the Harvard Forest to gain a better understanding of the processes that may be responsible for advecting CO₂ away horizontally from a given place in a forest.

Several groups have recently attempted to measure horizontal advection (Aubinet et al., 2003; Anderson and Turnipseed, 2001; Staebler et al., 2002, 2001, 2000). Aubinet et al. (2003) showed results from three summer months when there was evidence of horizontal advection along what was assumed to be a 2D slope, associated with measurable entrainment of air from aloft. In their case, the horizontal advection term is mostly cancelled by associated vertical advection, i.e. the CO₂ converging horizontally into the “control volume” is advected vertically out of the box, and the net effect on the NEE is small.

Anderson and Turnipseed (2001) have estimated the advection flux down the slope at an alpine forest in Colorado. They also assume 2D motion. The advective fluxes were noisy, and have not been compared to the vertical eddy flux.

Even on a well-defined slope, it may be risky to assume that there is no lateral motion or divergence that can transport CO₂ without demonstrating this by measurement. In addition, the study of idealized situations may lend itself to easier interpretation, but applicability of the results to more typical situations may be questionable.

Some studies have inferred the advective flux indirectly. Sun et al. (1998) published evidence of the significance of horizontal advection of CO₂ by showing increased concentrations over a lake at night and in the early morning, inferred to be due to nocturnal advection of respired CO₂ from the surrounding forests by land-breeze circulation. They estimated advection of CO₂ that roughly agreed with general estimates of respiration, although respiration rates for that night were not confirmed. The results were based on a data collected over a single lake on a single morning, and there was no direct observation of subcanopy advective flows, making generalization difficult.

Eugster and Siegrist (2000) attributed the difference between the flux estimated by boundary layer accumulation of CO₂ and the surface eddy flux to horizontal advection. Based on data from two nights, they found that advection was an order of magnitude larger than the local vertical eddy flux. Yi et al. (2000) in-

ferred the horizontal advection of CO₂ by calculating the vertical flux divergence between levels on a tall tower, and found advection to account for 27 and 5% of diurnally integrated NEE values between levels of 30 and 122 m, and 122 and 396 m, respectively.

All these studies agree on the high variability of the measured or inferred horizontal advection. It is clear that long averages are required to obtain meaningful results. In this study, 3D data over 2 years for nights of similar characteristics were composed to obtain statistically meaningful averages.

To show in a systematic manner that subcanopy advection is a significant effect, several steps are necessary.

- First, it must be shown that systematic subcanopy flows exist, and that they are measurable. In the published literature up to this point, this has simply been asserted but not demonstrated (e.g. Baldocchi et al., 2000; Goulden et al., 1996).
- Second, these flows must be related to a physical driving mechanism that ensures that they are systematic. This also provides a means towards generalization and modeling.
- Third, a methodology must be developed to determine the appropriate network size to capture the relevant gradients and transport processes, and to compose sufficiently long averages to counteract the expected small size of the signal.
- Finally, it must be demonstrated that the CO₂ gradients and transport processes in the subcanopy conspire to produce mean net transport of CO₂ into or out of the control volume under observation.

Section 2 will first review the assumptions underlying standard eddy covariance methods. The measurements conducted will be described in 2.2, followed by an outline of the methods used to integrate the horizontal measurements vertically in 2.3, and to determine horizontal heterogeneity and the appropriate size of the subcanopy network in 2.4. Section 2.5 will provide an estimate of the magnitude of the turbulent horizontal flux divergence. Two-layer budgets of CO₂ are discussed in 3.1, followed by a summary of the statistics of flux deficit nights in 3.2. In Section 3.3, measurements of horizontal advection of CO₂ will be shown. Section 4 summarizes the methodology and the results. To gauge the role of horizontal advection in the CO₂ budget, the contribution of the advection

terms during nights when the standard vertical flux method fails to detect the expected rate of respiration (“deficit nights”) are compared to the contribution on nights when the standard method provides reasonable estimates. If the horizontal advection of CO₂ accounts for the missed flux, the sums of all components should be invariant between the two sets of data.

2. Methods

2.1. The CO₂ budget

The equation for the conservation of a scalar c after Reynolds averaging is given by

$$\frac{d\bar{c}}{dt} = \frac{\partial \bar{c}}{\partial t} + \bar{u}_i \frac{\partial \bar{c}}{\partial x_i} + \bar{c} \frac{\partial \bar{u}_i}{\partial x_i} + \frac{\partial \overline{u'_i c'}}{\partial x_i} = \bar{s} \quad (1)$$

where s is the sum of sources and sinks, the overbars denote time averages, the primes denote departures of the instantaneous values from the time averages, and Einstein summation notation is used with $i = 1, 2, 3$ representing x, y and z directions. The molecular diffusion term is left out because it is several orders of magnitude smaller than the other terms.

The net ecosystem exchange (NEE) is defined as the flux through a horizontal plane at height h , i.e. the exchange rate between the forest (including the soil) and the atmosphere:

$$NEE_h = F_0 + \int_0^h \bar{s} dz \quad (2)$$

where F_0 is the soil flux entering (or leaving) the control volume at the bottom, and the integral describes the sum of all sources and sinks in the canopy space. Substituting Eq. (1) into (2), assuming incompressibility and simplifying to 2D for expediency results in

$$\begin{aligned} NEE &= F_0 + \int_0^h \frac{\partial \bar{c}}{\partial t} dz + \int_0^h \bar{u} \frac{\partial \bar{c}}{\partial x} dz + \int_0^h \bar{w} \frac{\partial \bar{c}}{\partial z} dz \\ &\quad + \int_0^h \frac{\partial \overline{u'c'}}{\partial x} dz + [(\overline{w'c'})_h - F_0] \\ &= \int_0^h \frac{\partial \bar{c}}{\partial t} dz + \underbrace{(\overline{w'c'})_h}_{[2]} + \int_0^h \bar{u} \frac{\partial \bar{c}}{\partial x} dz \\ &\quad + \int_0^h \bar{w} \frac{\partial \bar{c}}{\partial z} dz + \int_0^h \frac{\partial \overline{u'c'}}{\partial x} dz \end{aligned} \quad (3)$$

In common practice, only terms [1], storage, and [2], the vertical eddy flux at $z = h$, are considered, and all the other terms are assumed insignificant due to horizontal homogeneity. Term [4], the vertical mean advection, was proposed to be significant by Lee [1998], and can be calculated at the standard flux sites consisting of eddy covariance and profile instrumentation. In this paper, terms [3] and [4] will be evaluated and term [5] estimated indirectly.

Term [4] is integrated using the method in Lee (1998). First, the wind data have to be rotated such that the vertical velocities represent departures from the mean streamlines, which will be a function of the local topography. The measured vertical velocity \bar{w}_m is assumed to be made up of $\bar{w}_m = \bar{w} + a(\phi) + b(\phi)\bar{u}$, where $a(\phi)$ and $b(\phi)$ are coefficients determined by linear fits of \bar{w}_m against the wind speed u for 15° sectors of the wind direction ϕ , over the whole study. This method implicitly assumes that \bar{w} , the “real” vertical velocity which is the difference between the measured value and the average topographical streamline component, averages out to zero over such long times. Lee’s method then assumes that horizontal divergence is constant below h , which leads to a linear increase of \bar{w} with height, i.e. $\partial \bar{w} / \partial z \approx \bar{w}(h)/h$. Then, term [4] can be integrated by parts to yield

$$[\bar{w}\bar{c}]_0^h - \frac{\bar{w}(h)}{h} \int_0^h \bar{c} dz = \bar{w}(h) \left(\bar{c}(h) - \frac{1}{h} \int_0^h \bar{c} dz \right) \quad (4)$$

Measurements at Harvard Forest showed that the assumption of linear increase of \bar{w} with height is often violated (Staebler, 2003). Based on comparisons of the divergence measurements at 1.8 m with the measured vertical velocities at 8, 17 and 29 m, there is evidence that lower layers are often decoupled from those above. Generally, the divergence decreases faster with increasing height than the linear model would predict. However, we apply Lee’s formulation to provide an upper estimate of the vertical advection term in order to compare its potential significance relative to the other terms.

The method of vertical integration of the horizontal advection (term [3]) will be explained in Section 2.3.

2.2. Measurements

Measurements were made at Harvard Forest (Petersham, MA, 42°32'N, 72°11'W, 340 m MSL) for study periods in 1999, 2000, 2001 and 2002. This site is moderately hilly, with topographic gradients ranging from local slopes of 0.08 (80 m/km) towards the southwest (within 30 m), to 0.03 towards the west on a scale of 500 m and 0.09 towards the north on a scale of 1 km, thus presenting several scales for potential drainage flows.

Details of the permanent instrumentation at Harvard Forest can be found elsewhere (Moore et al., 1996). Eddy fluxes of CO₂ were available from the 29 and 8 m levels on the main tower. For this work, additional instrumentation was deployed in the subcanopy. The existing CO₂ profile was augmented by a 10-level profile in the lowest 5 m (Fig. 1). The existing temperature and humidity profiles on the main tower were augmented by an additional three levels on the 5 m tower.

After exploratory observations in 1999 that established the dominant subcanopy flow characteristics, horizontal CO₂ gradients were first measured in late 2000. The finalized network design was implemented in September 2001, and data was collected until December 2002, with an interruption between December 2001 and April 2002.

The final network design (see Fig. 2) consisted of six subcanopy sonic anemometers, with a Gill HS (Gill Instruments Ltd.) in the center of the grid and five SPAS/2Y (Applied Technologies Inc.) anemometers, with a resolution of 0.01 m/s, along the periphery. Horizontal gradients of CO₂ were measured by sampling sequentially from eight points surrounding the central location at distances of 40–60 m, and one point in the center in a 3 min cycle. The air was drawn through 9 mm i.d. Dekoron (Type 1300) tubes from meshed inlets to a manifold in a centralized box. A baseline air flow of 4 LPM from the inlets to a central manifold was maintained in all lines at all times to ensure relatively “fresh” air was being sampled. At the manifold, one line at a time was then sampled using an infrared gas analyzer (Licor, 7000). The 10-level CO₂ profile on the 5 m tower was determined in a similar, sequential manner, using a Licor 6262 gas analyzer. Flow rates at the inlets were checked regularly to ensure proper flow and to detect potential leaks.

2.3. Integrating the advection terms vertically

To use the horizontal measurements in a budget, they must be integrated vertically (as in Eq. (3)). However, it is often not feasible to obtain vertical profiles of these horizontal gradient measurements, i.e. to bound a complete 3D box with measurements. To address

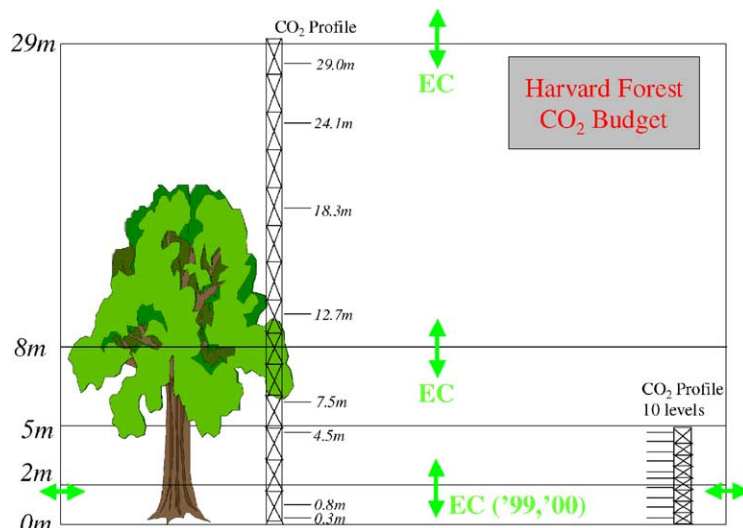


Fig. 1. Schematic representation of the CO₂ measurements at the Harvard Forest. EC denotes eddy covariance.

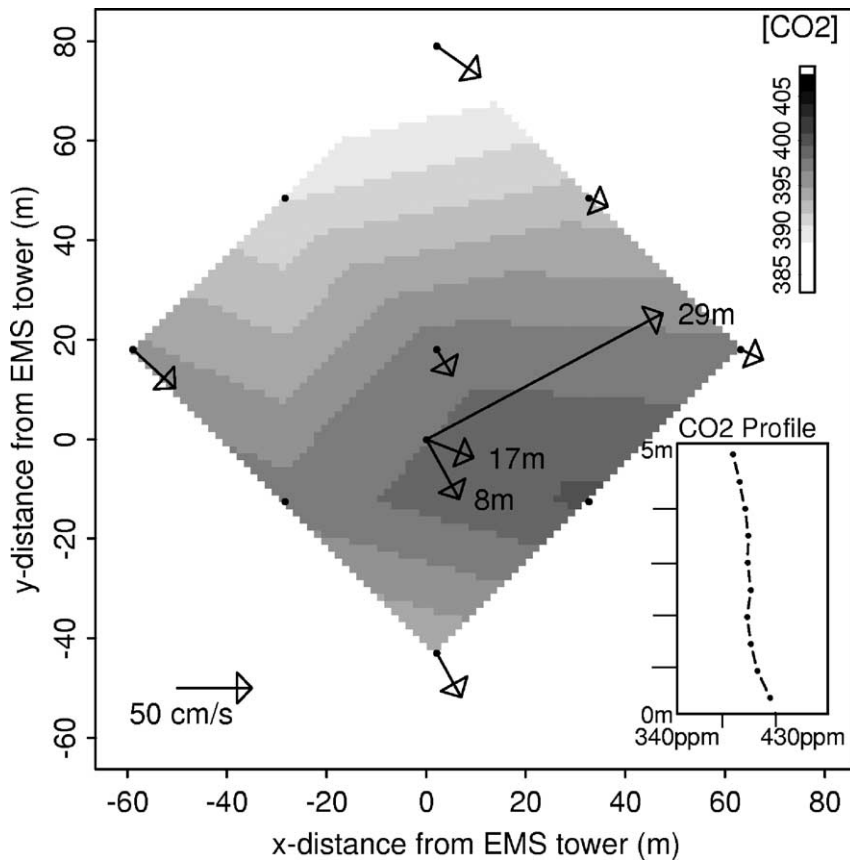


Fig. 2. Experiment layout. Shown is a 6 min average on the night of DOY 294 (19 October 2001) at 2:19EDT, of the wind vectors at the 9 sonic anemometer locations, an interpolated $[\text{CO}_2]$ field based on measurements at 9 points around the perimeter and in the center of the diamond. The inset shows the simultaneous CO_2 profile measured at the center of the square; tick intervals are 30 parts per million (ppm) (abscissa) and 1 m (ordinate). Wind vectors from the three tower anemometers are labeled by their height above ground.

this problem, we assert spatial similarity among vertical profiles of $[\text{CO}_2]$, the wind speed and their product uc (the horizontal transport), i.e. that the shapes of the profiles at all the horizontal end points are similar to that in the middle, where an actual profile is being measured. Physically, similar profiles would result from horizontal homogeneity of the vertical diffusive processes away from the surface as well as the sources and sinks in the canopy space. Based on the data, this can be justified by the fact that the normalized profiles collapse to well-defined shapes regardless of wind direction, wind speed or thermal conditions, as shown in Fig. 3. Horizontal CO_2 gradient measurements in 2000 also support the validity of extrapolating single level measurements; in that year, CO_2 concentrations

were integrated vertically (0.5–1.8 m) and horizontally (7 m width) at the north and south ends of the network, weighted more heavily closer to the ground. These spatially averaged gradients compared well with the single-level gradients in 2001 in sign and magnitude, as a function of the time of day as well as the wind speed.

Fig. 3 also shows that the horizontal array height is near the peak of the product, i.e. the height where the advection term is strongest. This gives some confidence in using measurements at a single height to determine the integrated layer advection.

To explain formally the process of integrating up, we invoke a similarity hypothesis and assert that the CO_2 profile at any point throughout the area of interest

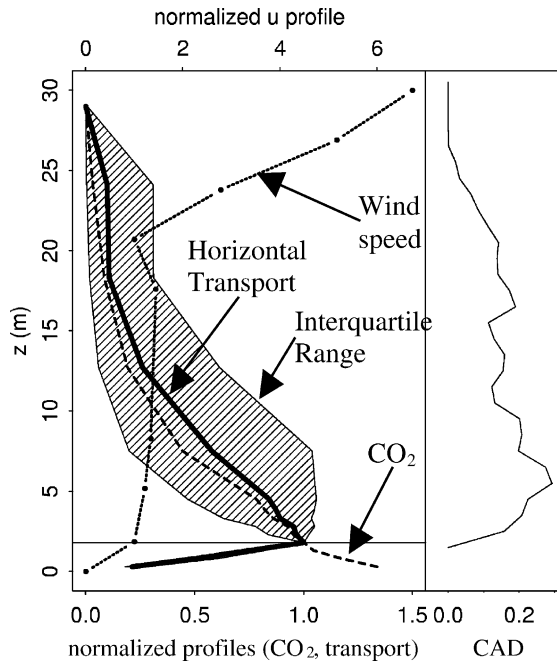


Fig. 3. Median profiles of CO_2 , the wind speed, and their product, representative of the profile of the horizontal transport, all normalized with respect to their values at the horizontal network level (1.8 m above ground). The shaded region denotes the interquartile range for this term. The horizontal line at $z = 1.8$ m marks the height of the horizontal measurement array. The wind speed at 21 m is probably an underestimate due to instrument defect, but this does not significantly affect the transport shape factor. The right panel shows the summer canopy area density profile (CAD [m^{-1}]).

is given by

$$c^*(x, z) = f(z)c^*(x, z_1) \quad (5)$$

where $f(z)$ describes the shape of the CO_2 profile, the reference height $z_1 = 1.8$ m, and $c^*(z) = c(z) - c_0$, i.e. the difference between the concentration and a baseline value. c^* is used instead of c because there is a practical lowest limit of $\text{CO}_2 = c_0$, indicative of the atmospheric base state, which can be separated from these calculations since it has no effect on the budget. The nocturnal CO_2 concentration above the canopy was used as this baseline value.

Vertical integration then gives

$$\begin{aligned} \int_0^h \frac{\partial c^*(x, z)}{\partial x} dz &= \frac{\partial c^*(x, z_1)}{\partial x} \int_0^h f(z) dz \\ &= \frac{\partial c^*(x, z_1)}{\partial x} h S_c \end{aligned} \quad (6)$$

where S_c is the shape factor for the CO_2 concentration profile.

The same argument can be made for the wind speed profile. The two can then be combined to yield

$$\begin{aligned} &\int_0^h u(x, z) \frac{\partial c^*(x, z)}{\partial x} dz \\ &= \int_0^h g(z) u(x, z_1) f(z) \frac{\partial c^*(x, z_1)}{\partial x} dz \\ &= \left(u(x, z_1) \frac{\partial c^*(x, z_1)}{\partial x} \right) \int_0^h f(z) g(z) dz \\ &= \left(u(x, z_1) \frac{\partial c^*(x, z_1)}{\partial x} \right) (hS) \end{aligned} \quad (7)$$

where S is the shape factor for horizontal advection of CO_2 . At night, this shape factor averaged 0.25 ± 0.13 (standard deviation; standard error was 0.003) in the fall of 2001, and 0.26 ± 0.15 (S.E. 0.003) for the 2002 growing season. Daytime values are typically ~ 0.15 , and there are no significant seasonal trends. To establish the time series of the vertically integrated horizontal advection, the discrete half-hour average profiles of CO_2 were used.

2.4. Horizontal heterogeneity

It is reasonable to question whether horizontal heterogeneity in both the wind field and the CO_2 sources near the ground inside a forest would make it impossible to make representative measurements with a small network. There may be significant local variations in the wind field due to obstacles such as trees and shrubs, as well as localized topography such as creeks and mounds, and wind measurements at the anemometers locations may be biased due to these obstacles. In some cases, stations may actually be located in different, decoupled airsheds. CO_2 concentrations near the ground reflect respiration rates, especially at lower wind speeds, and these vary depending on soil composition, temperature and moisture.

The effects of obstructions on the subcanopy wind field are discussed in Staebler (2003). A study by Wilson and Meyers (2001) examined the variability of fluxes both horizontally and vertically at the floor of a deciduous forest. Some variability in both wind speed and direction exists in the subcanopy flow field due to the various obstacles in the understory. Advection

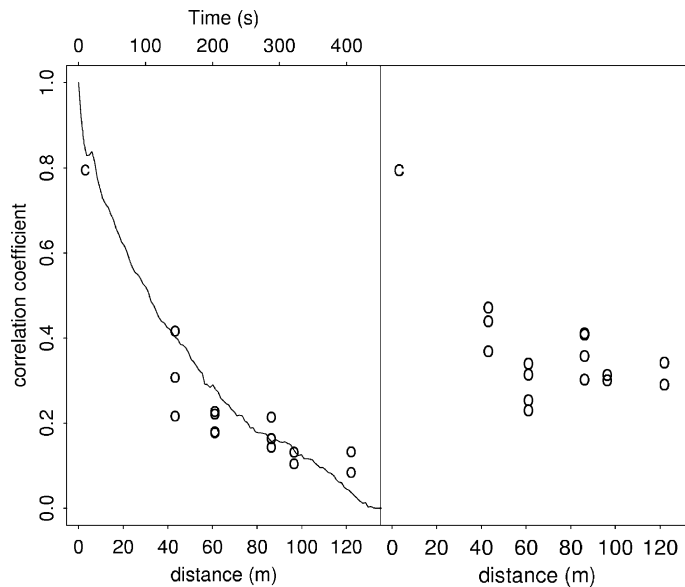


Fig. 4. The correlation coefficient for wind speeds (left panel) and CO₂ concentrations (right panel) as a function of distance between sampling points, for 3 min averages from DOY 150–330, 2002, represented by open circles. *c* Represents the calibration period when all sensors were collocated. The line in the left panel is the single-point autocorrelation (data from 2000) and corresponds to the axis at the top. The bottom and top axes are equivalent given the median subcanopy wind speed of 0.3 m s^{-1} .

values reported here are based on the average wind vectors of the anemometers in the network.

For the subcanopy array to qualify as a “network”, signals at the individual points have to be correlated, i.e. their spacing must be on the order of the relevant scales of transport or smaller. The autocorrelation for CO₂ was determined early in the study from continuous measurements at a single point (Fig. 4). These calculations indicate that the relevant time scales are on the order of 100–400 s. Translating this to a spatial scale using Taylor’s hypothesis ($X = UT$) results in a range of 40–160 m, given corresponding wind speeds. The applicability in this context is demonstrated below. This estimate agrees with a published estimate of the separation between adjacent coherent structures of 6–10 h, i.e. 120–200 m, at the same forest (Lu and Fitzjarrald, 1994). These values figured into both the spatial design of the array as well as the sampling period chosen (a 3 min cycle to rotate through the nine points).

The true test of this estimate, and whether the array is a network for practical purposes, was to examine whether the spatial correlations, determined once the array was in place, agreed with the correlations

predicted by conversion of the temporal to a spatial correlation. The 3 min data were high-pass filtered by subtracting a 1 h running mean in order to concentrate on fluctuations in CO₂ and wind speed that were unbiased by the much stronger diurnal cycles. These diurnal cycles force a very strong correlation, but this correlation is not a measure of spatial coherence on the scale of interest, since it would be strong even between completely separated forests, connected only by the common diurnal cycle of solar radiation and its resultant meteorological conditions. This filtered spatial correlation decreases with distance as shown in Fig. 4 and agrees well with the temporal estimate. We conclude that the spacing of network points represents about one spatial integral scale, and that Taylor’s hypothesis is actually applicable in this context.

The calibration period (day of year (DOY) 330–338, 2002) provided an estimate of the systematic errors to be expected in the horizontal CO₂ field measurements. A comparison of this period with the 8 days of actual measurements just prior showed that the standard deviation amongst the inlets dropped from 1.6 ppm (DOY 322–330) to 0.16 ppm (DOY 330–338), and that systematic offsets, caused by

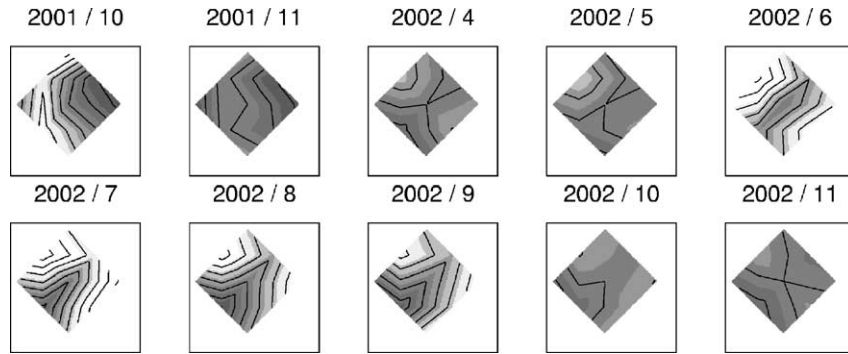


Fig. 5. Monthly mean nocturnal CO₂ concentration fields, relative to the concentration at the center. The diamond covers the same area as shown in Fig. 2. Contour lines have a spacing of 1 ppm; lighter colors indicate higher concentrations.

sequentially sampling a continually changing signal, were smaller than 0.3 ppm. Any seasonal variations above a potential systematic offset of 0.3 ppm were therefore thought to be a true representation of actual horizontal concentration differences.

Horizontal heterogeneity in the CO₂ field varied significantly from 2001 to 2002 (Fig. 5). In the fall of 2001, CO₂ concentrations were, on average, highest at the *E* end of the array, inside the hemlock stand. For most of 2002, they were highest near the *S* and *SW*. The reason for this may have been inter-annual differences in soil moisture: during field inspection of the inlets it was noted that the area surrounding the *SW* inlet was relatively wet early in the summer of 2002 compared to the previous year. According to Savage & Davidson (2001), upland (dry) soils at the Harvard Forest can increase their respiration rates when wet, and respiration rates at a single site can vary by a factor of 2 from year to year.

Due to the strong vertical gradient of CO₂ near the ground, it should be confirmed that persistent horizontal gradients observed are not just due to differences in the heights of the inlets relative to ground. The inlets were all at the same height above ground within ± 5 cm. The median vertical gradient from 1 to 2 m above the surface is ~ 2 ppm m⁻¹, which produces a concentration uncertainty of ± 0.1 ppm, clearly much smaller than the consistent differences of several ppm that are seen horizontally (Fig. 5).

Pooling of CO₂ in lower-lying areas, and especially bowl-shaped depressions, could also contribute to persistent horizontal gradients. However, we contend that, regardless of the physical origins of a horizontal gradi-

ent of CO₂, if it coexists with air motion along the direction of the gradient, then there is horizontal movement of CO₂, i.e. an advective flux. Even though it may be tempting to remove the mean gradients to obtain a filtered version of the (perturbation) advective fluxes, this is not done here because the gradients are believed to be real within ± 0.3 ppm. There is no a priori reason to insist that horizontal gradients and thus advection magnitudes and directions may not change from year to year, depending on the respiration characteristics of the various contributing patches of soil, which may vary according to inter-annual changes in soil moisture, composition or temperature.

2.5. Turbulent horizontal flux

The turbulent horizontal flux of CO₂ (term [5] in Eq. (3)) deserves some attention. Finnigan (1999) argued that this term is probably small based on a linear model of flow over a forested hill (Raupach et al., 1992). No direct measurement of the term is available because the long sample tubes make direct correlation of wind speed with CO₂ concentration difficult. However, direct measurements of the horizontal flux divergence of temperature ($\partial u'T'/\partial x$), available from the 1 s sonic anemometer data, can be compared to the vertical flux divergence as well as to the mean advection of temperature, $\partial \bar{u}\bar{T}/\partial x$, in order to determine their relative sizes. To perform the vertical integration, it was assumed that $(\partial u'T'/\partial x)_{29\text{m}} \approx [(w'T')_{29\text{m}}/(w'T')_{1.8\text{m}}](\partial u'T'/\partial x)_{1.8\text{m}}$, and that linear interpolation between the 29 m and 1.8 m levels was sufficient for this order-of-magnitude estimate.

The horizontal eddy flux divergence was found to be usually no more than 10% of the vertical flux, and less than $\sim 30\%$ of the mean advection.

Another method of estimating the horizontal eddy flux is to employ the relationship between eddy covariance and the product of the standard deviations, $\overline{u'c'} = r_{uc}\sigma_u\sigma_c$, where r_{uc} is the correlation coefficient between the two parameters. This can be related to the temperature covariance by $\overline{u'c'} = (r_{uc}/r_{uT})(\sigma_c/\sigma_T)\overline{u'T'}$. Applying a measured slope relating c to T of about -290 ppm/K, representative of warm summer nights, the flux estimate $\partial\overline{u'c'}/\partial x \sim (290 \text{ ppm/K})\partial\overline{u'T'}/\partial x$ provides an estimate of about $1 \mu\text{mol m}^{-2} \text{ s}^{-1}$, which is the order of magnitude of the mean horizontal transport (see further) and certainly significant. This estimate is probably near the upper limit because the slope is a factor of the vertical gradients of both the CO_2 and temperature, and because vertical gradients of CO_2 are significantly larger during the summer than in the peripheral seasons. Since these measurements are the first of their kind and there are no guidelines in the literature on how to treat the turbulent advection of CO_2 , we only note that these terms may be significant enough to warrant further study, but neglect them in the subsequent analysis.

3. Results

3.1. Layer budgets

An estimate of the expected upper limit of the advective flux can be obtained by constructing layer-averaged budgets of CO_2 based on available measurements. Although not all components are measured at all times, continuous eddy flux measurements at 8 and 29 m are available, as well as the CO_2 profile. If some reasonable estimates are made of the respiration from the soil, stems and leaves, then the two layers from 0 to 8 m and from 8 to 29 m can be evaluated (Fig. 1).

The currently most frequently employed approach to dealing with the nocturnal flux problem is to establish a lower limit of the friction velocity, u_* , above which the turbulence is deemed sufficient to completely capture the flux by EC (Pattey et al., 2002). Below this “ u_* -cutoff” the measured (but presumably incorrect) fluxes are replaced with proxy values

derived from auxiliary data. Most commonly, it is assumed that the forest respiration rate is mainly a function of soil temperature, and sometimes also soil moisture (Savage and Davidson, 2001), and the nocturnal flux is calculated using a fit of EC fluxes versus soil temperatures during conditions of sufficient u_* .

As a result of this “gap filling”, what is often mistakenly perceived as real data from direct measurements is actually a composite of real and surrogate data, the latter often representing a fraction of 30–40% (Goulden et al., 1996; Greco and Baldocchi, 1996; Falge et al., 2001). Moreover, it is often not clear where the u_* cut-off should be placed, and the resulting uncertainty can be large enough to change a forest from a net sink to a net source [Miller et al., 2003]. This approach is not very satisfying in a physical sense, since it employs empirical relationships as soon as the simplified physical description of forest–atmosphere exchange fails.

To examine the consequences of this practice, “expected” flux rates (F_{exp}) based on soil temperatures were calculated for nocturnal fluxes satisfying $u_* > 0.2 \text{ ms}^{-1}$. A slight modification that produced better agreement between estimated respiration and NEE on non-deficit nights was to fit the 75th percentiles of the respiration rate, separated into 0.2 bins of soil temperature, to the soil temperature, rather than the mean or median (Fig. 6). The u_* criterion fails to eliminate a good fraction of the deficit nights (see further). Fitting the mean or median results in an underestimate of the respiration on non-deficit nights, and we end up with many nights where there seems to be a surplus in respiration. Using the 75th percentile approximates the fit that would be obtained by connecting the plateaus of nights when NEE appears to detect all the respiration (see further). It also agrees better with estimates based on 4 years of chamber data collected by Savage and Davidson in the vicinity of the Harvard Forest tower (Savage and Davidson, 2001). The resulting exponential fit explains 14% of the variance (Fig. 6). This is a very low, but not uncommon value (Hollinger et al., 1994; Lavigne et al., 1997; Goulden et al., 1996).

The estimated respiration rates depend to some extent on where the u_* cut-off is placed. As seen in Fig. 7, this is not always obvious. Sometimes, a distinct plateau is reached as u_* increases, while at other times, the NEE continues to increase, making it difficult to determine a point above which the eddy

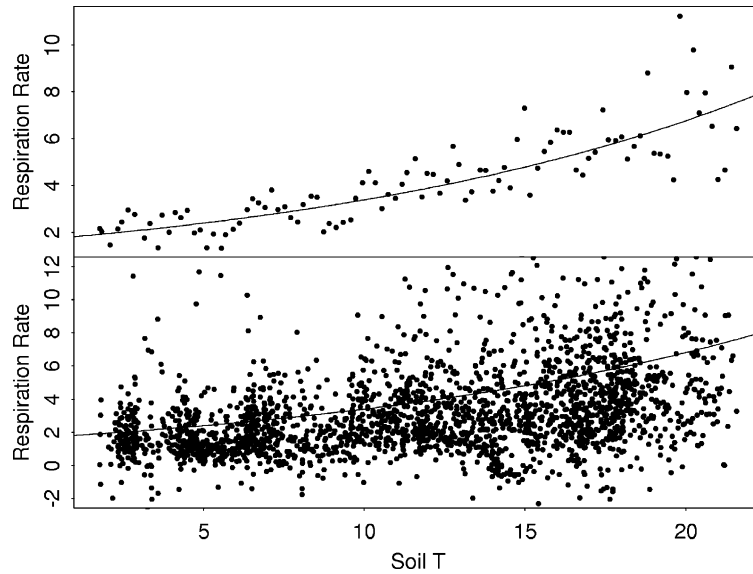


Fig. 6. Top: Fit of nocturnal NEE against soil temperature, binned into 0.2° blocks ($r^2 = 0.74$). Bottom: The exponential fit to the population of half-hour NEE data ($r^2 = 0.14$). Respiration rates are in $\mu\text{mol m}^{-2} \text{s}^{-1}$, temperatures in $^\circ\text{C}$.

covariance supposedly captures the whole flux. Complications arise at higher u_* because hypothesized “pressure pumping effects” may physically increase respiration rates due to improved venting of air capillaries in the soil (Malhi et al., 1999). If this effect be-

comes significant at different u_* at some sites, it may explain the lack of a distinct plateau. Further complications can arise at higher u_* , such as low frequency of occurrence or seasonally biased occurrence. The drop of NEE at higher u_* at Borden is mainly explained by

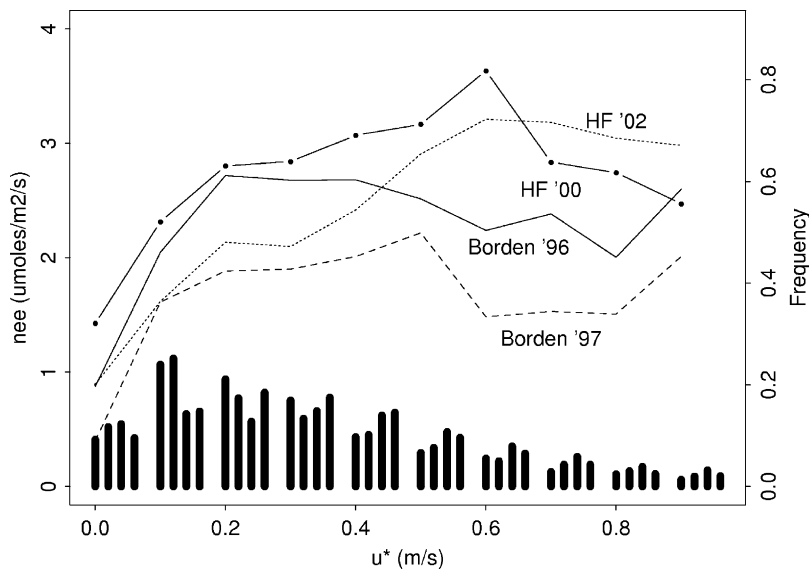


Fig. 7. NEE vs. the friction velocity u_* at Harvard Forest and Borden for 2 years each. The bars represent the frequency of occurrence of a given range of u_* values in chronological order for the four curves.

the higher frequency of large u_* during the leafless period, when respiration is lower than during the foliated season. In general, however, both Harvard Forest and Borden are reasonably well-behaved, and the standard approach would impose u_* cut-off limits at about 0.2 ms^{-1} .

Direct measurements of leaf and stem respiration were not made, but are between 20% (Wofsy et al., 1993) and 32% (Goulden et al., 1996) of soil respiration at this site, the leaves contributing 28% and the stems 5%. Based on measurements of the canopy profile, 57% of the canopy lies above 8 m, and scaling linearly results in an estimated canopy respiration rate of about 20% of the soil respiration rate during foliated periods and 4% during leafless periods.

For November 2001 (DOY 300–330), the nocturnal budget in the 8–29 m layer closed to $-0.07 \pm 0.2 \mu\text{mol m}^{-2} \text{ s}^{-1}$ and the 0–8 m layer to $-0.35 \pm 0.2 \mu\text{mol m}^{-2} \text{ s}^{-1}$ (negative values indicating either an unaccounted sink in the layer or transport out of it). If we were to assume that this was due to horizontal transport, the larger imbalance in the bottom layer agrees with the shape factor calculations, which suggest that 75% of the horizontal transport occurs below 8 m. In the top layer, by far the most significant terms are the flux into the layer from below at 8 m and the flux out of the layer at 29 m, which are practically equal. The flux out of the bottom layer at 8 m almost accounts for the estimated soil respiration.

For the summer months in 2002, the nocturnal budget in the top layer had a surplus of $0.9 \pm 0.3 \mu\text{mol m}^{-2} \text{ s}^{-1}$ and the bottom layer a deficit of $-1.6 \pm 0.2 \mu\text{mol m}^{-2} \text{ s}^{-1}$, using the above apportionment of respiration amongst leaves, stem and soil (16, 4, 80%). If leaf respiration is eliminated in the top layer, these values shift to 0.06 ± 0.3 and $-2.4 \pm 0.2 \mu\text{mol m}^{-2} \text{ s}^{-1}$, respectively. A possible explanation for the surplus in the top layer in the first estimate would be the overestimation of leaf respiration. Previous results (Goulden et al., 1996) for this site were based on a few weeks of leaf chamber studies during August, and are probably not representative of the whole growing season.

Regardless of the details of the apportionment of respiration, there clearly is evidence of an imbalance, especially in the layer closer to the ground. This imbalance may be caused by CO_2 leaving the control volume horizontally, and determining whether

this is the case is discussed in the remainder of this paper.

3.2. Phenomenology of CO_2 flux deficits

The method of estimating the respiration rate, i.e. the expected nocturnal flux F_{exp} , was shown above. F_{exp} was then compared to measured EC fluxes plus storage, and the difference was defined as the “flux deficit” ΔF :

$$\Delta F = F_{\text{exp}} - \left((\overline{w'c'})_h + \frac{\partial}{\partial t} \int_0^h c(z) dz \right) \quad (9)$$

where the second term on the RHS is the EC flux at height h above ground, and the third term represents the rate of change of storage below h , c being the concentration of CO_2 . The equation also illustrates the commonly used definition of NEE as eddy flux plus storage.

To determine the situations under which flux deficits occur, all four study periods (1999–2002) were analyzed for coincidence of apparent deficits with potentially related meteorological parameters such as u_* , thermal stability in the canopy, net radiation, and wind speed and direction both above and below the canopy. The subcanopy flow can best be characterized by looking at the relative sizes of the three driving forces in the Boussinesq equation for momentum along a slope,

$$\begin{aligned} \frac{\partial u}{\partial t} + u \frac{\partial u}{\partial x} + w \frac{\partial u}{\partial z} \\ [1] \quad [2] \quad [3] \\ = -\frac{1}{\rho} \frac{\partial p^*}{\partial x} - g \frac{\theta_v^*}{\theta_v} \frac{\partial z}{\partial x} - \frac{\partial \tau}{\partial z} - F_D \end{aligned} \quad (10)$$

where ρ is the density, p^* the pressure perturbation, θ_v the virtual temperature, θ_v^* the local departure of θ_v from the mean, $\partial z/\partial x$ the topographic slope, τ the stress, F_D the canopy form drag, and only the vertical stress divergence is included. Forcing fractions are defined by calculating the absolute values of forcing terms [4]–[6],

$$t_a = \left| \frac{\partial \tau}{\partial z} \right|, \quad p_a = \left| \frac{1}{\rho} \frac{\partial p^*}{\partial x} \right|, \quad b_a = \left| g \frac{\theta_v^*}{\theta_v} \frac{\partial z}{\partial x} \right| \quad (11)$$

Details of the parameterization can be found elsewhere (Staebler, 2003). Briefly, p^* is estimated from the linear theory by Hunt et al. (1988), which predicts a maximum pressure gradient for a series of

sinusoidal 2D hills to occur halfway downhill in the lee of the peak and to have a maximum magnitude of $\partial p^* / \partial x \sim \rho U_0^2 (H/2)(\pi/2L)^2$, where U_0 is a reference wind speed aloft. θ^* represents the deviation of the potential temperature at height z from that above the forest at $z = 30$ m.

The “forcing fractions” are formed thus:

$$\begin{aligned} t\text{frac} &= \frac{t_a}{(t_a + p_a + b_a)} \\ p\text{frac} &= \frac{p_a}{(t_a + p_a + b_a)} \\ b\text{frac} &= \frac{b_a}{(t_a + p_a + b_a)} \end{aligned} \quad (12)$$

These fractions can indicate a dominance of the stress divergence, pressure forcing, and negative buoyant (drainage) forcing terms respectively. The process of selecting deficit nights is illustrated in Fig. 8. In

this 5-day period, 4 of the 5 nights suffer from flux deficits. The only night when NEE agrees well with the predicted respiration rate is 295, when the stress fraction dominates. Nights 292, 294 and 296 represent nights with the right conditions for drainage flows, and in all three cases subcanopy flows from the north are detected, despite different wind directions aloft. The deficit on 293 appears a little smaller, and is associated with a smaller thermal inversion inside the canopy. Note that u_* drops below its critical value (the dashed line at 0.2 ms^{-1}) only during 294 and the first half of 296, while remaining above 0.3 ms^{-1} most of 293. Also note that the net radiation is a useful indicator of thermal stability.

Table 1 summarizes the findings for the three study periods. On average, 58% of the nights studied display the problem of CO_2 flux deficits. Only 41% of these actually qualify as “calm” nights given the u_* criterion (0.2 ms^{-1}) established for this site by Goulden et al.

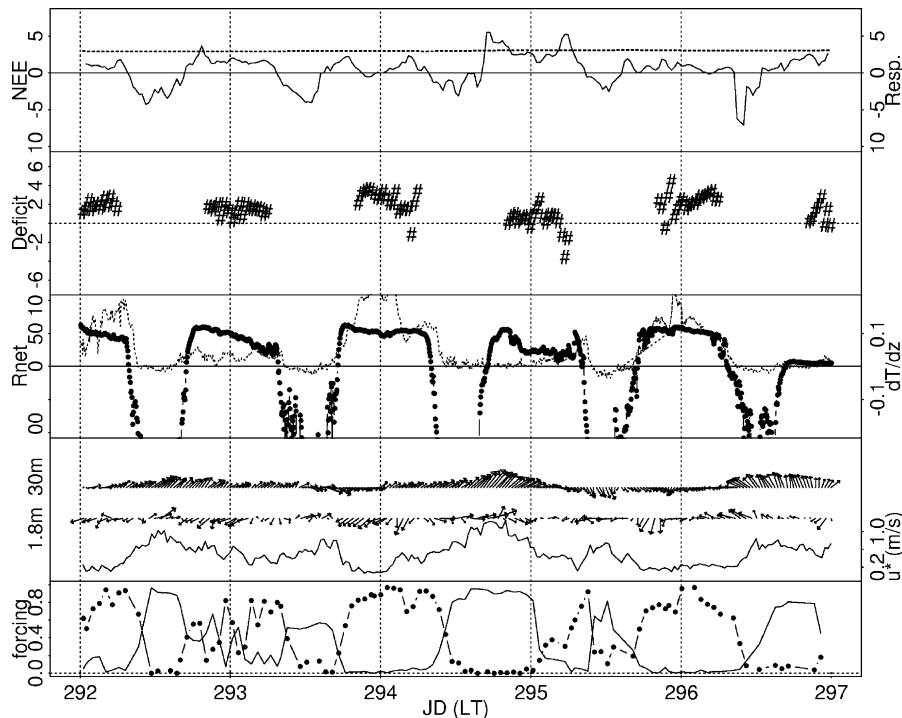


Fig. 8. Five days of data collected at the Harvard Forest in 2001. Vertical dashed lines are at midnight local time (EDT). The top panel shows the eddy flux plus storage correction (in $\text{mmol m}^{-2} \text{ s}^{-1}$, solid line) in comparison with the respiration rate expected based on soil temperature (dashed line). The second panel shows the difference between these two (i.e. the flux deficit). The third panel shows net radiation (W m^{-2} , dark line) and dT/dz ($^{\circ}\text{C m}^{-1}$, light line). The fourth panel shows the wind vectors at 29 and 1.8 m, in addition to the friction velocity at 29 m. The fifth panel shows the forcing term fractions $b\text{frac}$ (connected dots) and $t\text{frac}$ (solid line).

Table 1
Summary of nocturnal CO₂ flux deficit statistics

Study period	27 July–8 November 1999	22 August–24 November 2000	9 October–26 November 2001	19 April–4 December 2002	Total
Number of nights with all data	70	66	46	128	310
Number with CO ₂ flux deficit (<i>N</i>)	40 (57%)	38 (57%)	24 (52%)	79 (62%)	181 (58%)
Deficit night statistics					
Number of deficit nights with $u_* < 0.2 \text{ ms}^{-1}$	15 (38%)	15 (39%)	9 (38%)	36 (46%)	75 (41%)
Number of deficit nights with drainage flow	27 (68%)	27 (71%)	20 (83%)	51 (65%)	125 (69%)
Number of deficit nights with stress flow	1 (3%)	2 (5%)	0 (0%)	7 (9%)	10 (6%)
Number of deficit nights with pressure flow	10 (25%)	6 (16%)	4 (17%)	17 (22%)	37 (20%)

The last four rows refer to the subset of nights with CO₂ flux deficits. Note that the last three rows may not always add up to 100% because on some nights none of the forcing terms were clearly dominant.

(1996). Of the nights with CO₂ flux deficits, about 69% are associated with subcanopy flows that are generated by negative buoyancy, i.e. under drainage flow conditions. Therefore, the buoyant fraction is a superior predictor of deficit nights since it actually combines information on the relative significance of drainage flows and turbulent mixing.

In complex terrain such as at the Harvard Forest, the drainage flow direction is not obvious a priori, because flows have momentum which means that slopes below a certain scale may not develop gravity flows if nearby larger slopes overpower them. In stable conditions, multiple layers with different characteristics could be generated, and flows from different directions could overlay each other. Mahrt et al. (2001) observed that there can also be a temporal pattern with different drainage flow regimes dominating during different parts of the night.

Investigation of subcanopy flows under conditions of a strong buoyant forcing term indicated that drainage flows came predominantly from the north-west and north (Fig. 9). This is the direction of the longest uninterrupted slope on a scale of a few kilometer, not the steepest slope nor the slope in the immediate vicinity of the tower, which faces north-east. A similar drainage direction dependence on the longest slope was found at Borden (Staebler, 2003).

On 6% of deficit nights, the stress term appears to dominate, but often not for the whole night. Twenty percent of the deficit nights are associated with a dominant pressure forcing term, but since our estimate of this term is probably an upper limit, this fraction is probably an overestimate.

3.3. Estimates of horizontal advection

The time series of half-hour data of the measurable terms in the CO₂ budget for 2002 are shown in Fig. 10. Clearly the advection terms have similar seasonal cycles as the eddy flux, since all are dependent on the level of activity of the forest. Horizontal as well as vertical gradients of CO₂ are larger in

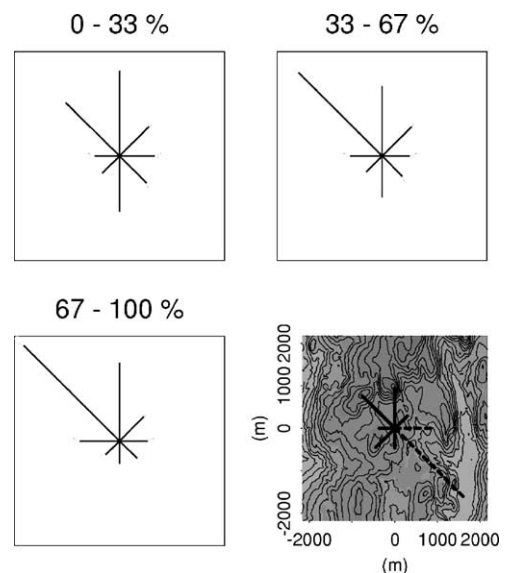


Fig. 9. Wind roses as a function of the fraction of the buoyant term in the sum of the forces, based on statistics for all data (8700 half-hours). The final panel shows a topographic map centered at the Harvard Forest flux tower. The dashed radials indicate the distance to the nearest hilltop (valley), i.e. the nearest significant topographic inflection point. The contour line interval is 15 m.

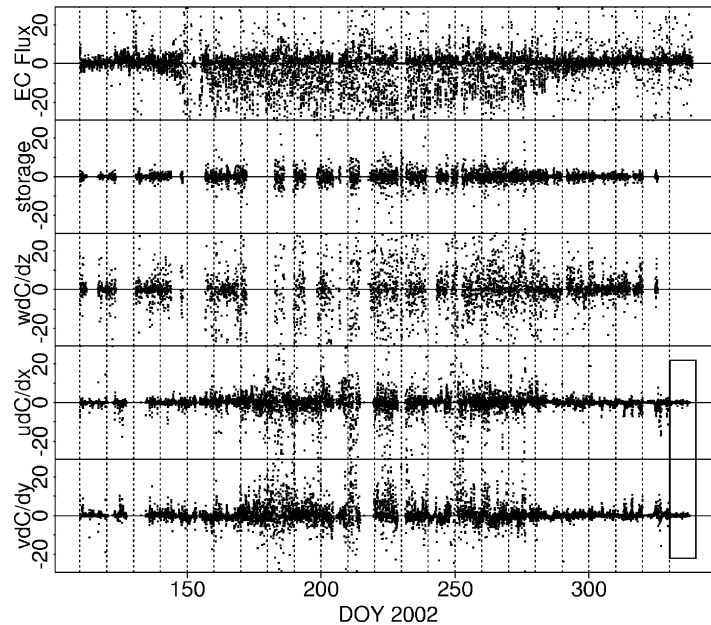


Fig. 10. Half-hour data for 2002 for the vertical eddy covariance flux at 29 m shown with the storage term, the vertical advection term, and the west-east and south-north horizontal advection terms, on identical scales. The period from day of year 330–335, indicated by the box, represents a calibration period with all inlets and anemometers collocated at the center of the grid. Units on the vertical axes are $\mu\text{mol m}^{-2} \text{s}^{-1}$.

the summer months, and this is reflected in all budget terms.

The variance of the advection terms is comparable in magnitude to the variance of the eddy covariance flux. While the seasonal pattern of uptake (negative flux) during the summer and respiration during the winter are apparent in the EC signal, there is no obvious seasonal pattern in any of the advective fluxes. However, when averaged over longer periods, values that are significantly different from zero are obtained. For both 2001 and 2002 at Harvard Forest, these make a positive contribution to the flux at this site (i.e. transporting CO_2 out of the “control volume” around the tower).

Fig. 10 also indicates the instrumental uncertainty associated with the measurements, in the calibration period from DOY 330–338. On DOY 330, all the CO_2 inlets and 2D sonic anemometers were brought back and collocated within 4 m of the center point (see Fig. 1), while data collection continued as previously. For the subsequent 8 day period, the west-east and south-north advection terms averaged to -0.05 ± 0.02 and $0.00 \pm 0.02 \mu\text{mol m}^{-2} \text{s}^{-1}$ respectively. As seen in

Fig. 11, averaging over about two nights is required to bring the standard error (between the two-night averages in this case) below $0.1 \mu\text{mol m}^{-2} \text{s}^{-1}$ during the calibration period. During the measurement periods, the standard error still decreases even after averaging over 30 nights. Clearly, short field campaigns will not suffice to determine the magnitude of the advection of CO_2 .

The average diurnal behavior of the terms, including their variability, is more clearly illustrated in Fig. 12. The storage term shows build-up of CO_2 in the forest in the evening (positive storage), which is then exhaled in the morning (between 7 and 11 EDT). The vertical advection term shows larger variance at night, when the vertical gradient of CO_2 is largest, but the median shows no clearly discernable diurnal trend. The horizontal transport terms also display larger variance at night due to increased horizontal CO_2 gradients. Note that there is a clearly positive offset in the north-south advection term, indicating transport out of the control volume in this direction. This term is associated with winds from the north and higher CO_2 concentrations at the southern end.

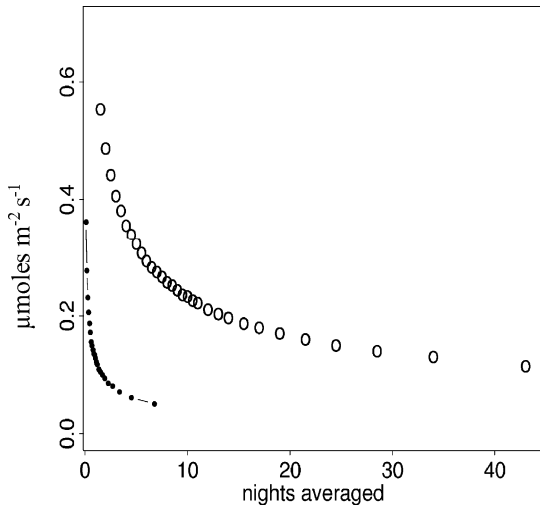


Fig. 11. The standard error on the advective flux as a function of averaging period (0). Only deficit nights in the 2002 period are included. The shorter line at the bottom left represents the calibration period in 2002 (i.e. the instrumental uncertainty) and includes daytime values.

To determine the relative contribution of the advection terms to the CO₂ budget, we compare nights with apparent flux deficits to nights without. If the total estimated NEE, including the advection terms, is invariant between these two sets of data, we can conclude that advection does indeed account for the CO₂ missed on deficit nights by the standard vertical measurements.

Results show that there is a resolvable difference in the magnitude of the advection terms between nights with CO₂ flux deficits (see Table 2 and Fig. 13) and those without. As expected, the eddy flux significantly decreased during deficit nights, while the storage term typically increased somewhat. On average, the vertical advection term appeared relatively insignificant

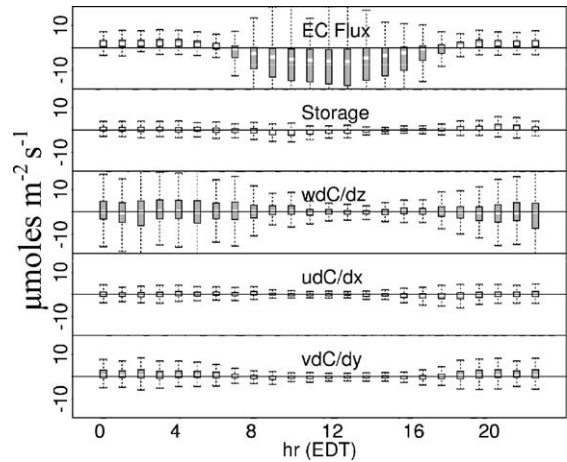


Fig. 12. Box plot of the diurnal cycle of the CO₂ budget terms for 2002. All fluxes are given in $\mu\text{mol m}^{-2} \text{s}^{-1}$. Boxes indicate the interquartile range, and the white stripe is the median. Outliers are given by the whiskers.

in all cases at this forest, although it contributes significant noise to the budget. The horizontal advection terms do contribute more to the budget during deficit nights, but apparently not enough to account for the difference in NEE on average. In the summer months, when larger signals prevail, closure between deficit and non-deficit nights is achieved to within the uncertainties, but in the transition periods, the sum of all components on deficit nights falls short of the sum on non-deficit nights. On average, the horizontal advection terms account for 35 and 13% of the CO₂ budget during deficit and non-deficit nights, respectively. However, the sum of all terms for deficit nights is still 32% short of the non-deficit total. Other transport mechanisms not dealt with here may contribute more significantly during transition periods. These mech-

Table 2
Summary of CO₂ budgets for all nights with complete data, 2001 and 2002

	Eddy flux	Storage	Vertical advection	Horizontal advection	Sum
Spring	1.1 ± 0.1 (3.2 ± 0.4)	0.37 ± 0.05 (0.39 ± 0.04)	0.0 ± 0.6 (0.0 ± 0.4)	0.4 ± 0.1 (0.2 ± 0.1)	1.9 ± 0.6 (3.8 ± 0.8)
Summer	1.7 ± 0.2 (3.3 ± 0.4)	0.84 ± 0.05 (0.83 ± 0.07)	0.2 ± 0.5 (-0.3 ± 0.6)	1.7 ± 0.2 (0.9 ± 0.2)	4.4 ± 0.6 (4.7 ± 0.8)
Fall	0.8 ± 0.1 (2.1 ± 0.4)	0.29 ± 0.02 (0.16 ± 0.03)	0.0 ± 0.2 (0.3 ± 0.2)	0.7 ± 0.1 (0.2 ± 0.1)	1.8 ± 0.2 (2.8 ± 0.5)
Total	1.3 ± 0.1 (2.6 ± 0.2)	0.47 ± 0.02 (0.38 ± 0.02)	0.1 ± 0.2 (0.1 ± 0.2)	0.94 ± 0.07 (0.45 ± 0.07)	2.8 ± 0.2 (3.5 ± 0.3)

Nights were segregated according to the criteria described in Table 1. The values without parentheses represent deficit nights, while the values in parentheses are non-deficit nights. The units are $\mu\text{mol m}^{-2} \text{s}^{-1}$.

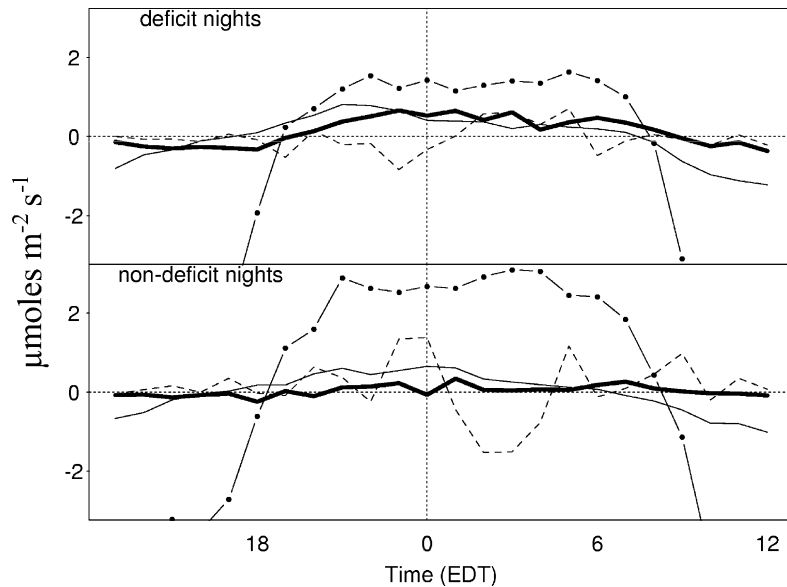


Fig. 13. Nocturnal CO₂ budgets for deficit and non-deficit nights. Connected dots: eddy flux at 29 m; thick solid line: the horizontal advection term; thin solid line: storage; dashed line: vertical advection term.

anisms include intermittent transport which is poorly dealt with by Reynolds' averaging [e.g. Massman and Lee, 2002], or transport on time scales that are either too fast or too slow to be captured by standard techniques sampling at 10 Hz and averaging over 30 min [Sakai et al., 2001].

4. Summary and conclusions

This work establishes a methodology to systematically determine horizontal advection of a CO₂ in the forest subcanopy. This methodology consists of determining the likely vertical extent of horizontal transport, establishing a network of sampling points that captures the relevant horizontal gradients while remaining correlated, and determining the methodological uncertainties involved. It has been shown that this type of measurement is feasible given current, off-the-shelf technology, if the data are integrated over long periods.

Direct measurements of horizontal advection of CO₂ in the subcanopy at the Harvard Forest indicate that this component contributes significantly to the transport of CO₂ under conditions when insufficient mixing results in an underestimate of respiration rates

by the standard eddy flux approach. Calm nights (when turbulent transport is low and the negative buoyancy near the ground strong) are associated with drainage flows from the north to north-west. These nights are well correlated with flux deficits, as well as with increased amounts of horizontal advection of CO₂.

These results do not preclude other effects from also contributing, such as intermittent transport which is poorly dealt with by Reynolds' averaging (e.g. Massman and Lee, 2002), or transport on time scales that are either too fast or too slow to be captured by standard techniques sampling at 10 Hz and averaging over 30 min (Sakai et al., 2001).

Out of 310 nights with complete data, 58% were associated with CO₂ flux deficits. Only 41% of these actually qualified as "calm" nights under standard ($u_* < 0.2 \text{ ms}^{-1}$) criteria. Of the nights with CO₂ flux deficits, about 69% were associated with subcanopy flows that were generated predominantly by negative buoyancy, i.e. under classic drainage flow conditions. Compared to the commonly used u_* criteria, the buoyancy forcing fraction was shown to be a superior predictor of deficit nights.

While the vertical mean transport term was shown to average close to zero on both deficit

and non-deficit nights, a significant difference of $0.49 \pm 0.14 \mu\text{mol m}^{-2} \text{s}^{-1}$ in the horizontal transport terms was observed. Including the mean transport terms did not account for the observed difference in NEE of $1.2 \pm 0.3 \mu\text{mol m}^{-2} \text{s}^{-1}$, but improved the CO_2 budget closure to $0.7 \pm 0.5 \mu\text{mol m}^{-2} \text{s}^{-1}$.

Acknowledgements

The authors gratefully acknowledge the assistance of Sasha Tsoyref, Matt Czikowsky, Otavio Acevedo, Kathy Moore, Gary Wojcik, Ricardo Sakai, Jeff Freedman, John Sicker and Dwayne Spiess with the field work. Bill Munger, John Budney and Steve Wofsy (Harvard University) made long-term measurements at the Harvard Forest possible by sharing their infrastructure and data. Behzad Abareshi wrote the software for the Linux data acquisition system. This research was supported by the Office of Science, Biological and Environmental Research Program (BER), US Department of Energy, through the Northeast Regional Center of the National Institute for Global Environmental Change (NIGEC), through a subcontract with Harvard University under Cooperative Agreement No. DE-FC03-90ER61010.

References

- Aubinet, M., Heinesch, B., Yernaux, M., 2003. Horizontal and vertical CO_2 advection in a sloping forest. *Bound. Layer Meteorol.* 108, 397–417.
- Anderson, D.E., Turnipseed, A.A., 2001. Estimating nocturnal respiration from profile measurements in a subalpine forest. *Eos Trans. AGU*, 82(47), Fall Meet. Suppl., Abstract B41A-12.
- Baldocchi, D.D., Finnigan, J.J., Wilson, K., Paw U, K.T., Falge, E., 2000. On measuring net ecosystem carbon exchange over tall vegetation on complex terrain. *Boundary Layer Meteorol.* 96, 257–291.
- Black, T.A., den Hartog, G., Neumann, H.H., Blanken, P.D., Yang, P.C., Russell, C., Nescic, Z., Lee, X., Chen, S.G., Staebler, R.M., Novak, M.D., 1996. Annual cycles of water vapour and carbon dioxide fluxes in and above a boreal aspen forest. *Global Change Biol.* 2, 219–229.
- Eugster, W., Siegrist, F., 2000. The influence of nocturnal CO_2 advection on CO_2 flux measurements. *Basic Appl. Ecol.* 1, 177–188.
- Falge, E., Baldocchi, D., Olson, R.J., Anthoni, P., Aubinet, M., Bernhofer, C., Burba, G., Ceulemans, R., Clement, R., Dolman, H., Granier, A., Gross, P., Grünwald, T., Hollinger, D., Jensen, N.-O., Katul, G., Keronen, P., Kowalski, A., Ta Lai, C., Law, B.E., Meyers, T., Moncrieff, J., Moors, E., Munger, J.W., Pilegaard, K., Rannik, Ü., Rebmann, C., Suyker, A., Tenhunen, J., Tu, K., Verma, S., Vesala, T., Wilson, K., Wofsy, S., 2001. Gap filling strategies for defensible annual sums of net ecosystem exchange. *Agric. Meteorol.* 107, 43–69.
- Finnigan, J.J., 1999. A comment on the paper by Lee (1998): on micrometeorological observations of surface-air exchange over tall vegetation. *Agric. Forest Meteorol.* 97, 55–64.
- Goulden, M.L., Munger, J.W., Fan, S.-M., Daube, B.C., Wofsy, S.C., 1996. Measurements of carbon sequestration by long-term eddy covariance: methods and a critical evaluation of accuracy. *Global Change Biol.* 2, 169–182.
- Hollinger, D.Y., Kelliher, F.M., Byers, J.N., Hunt, J.E., McSeveny, T.M., Weir, P.L., 1994. Carbon dioxide exchange between an undisturbed old-growth temperate forest and the atmosphere. *Ecology* 75 (1), 134–150.
- Hunt, J.C.R., Richards, K.J., Brighton, P.W.M., 1988. Stably stratified shear flow over low hills. *Q.J.R. Meteorol. Soc.* 114, 859–886.
- Lavigne, M.B., Ryan, M.G., Anderson, D.E., Baldocchi, D.D., Crill, P.M., Fitzjarrald, D.R., Goulden, M.L., Gower, S.T., Massheder, J.M., McCaughey, J.M., Rayment, M., Striegl, R.G., 1997. Comparing nocturnal eddy covariance measurements to estimates of ecosystem respiration made by scaling chamber measurements at six coniferous boreal sites. *J. Geophys. Res.* 102 (28), 977–985.
- Lee, X., 1998. On micrometeorological observations of surface-air exchange over tall vegetation. *Agric. Forest Meteorol.* 91, 39–49.
- Lu, C.-H., Fitzjarrald, D.R., 1994. Seasonal and diurnal variations of coherent structures over a deciduous forest. *Boundary Layer Meteorol.* 69, 43–69.
- Mahrt, L., Vickers, D., Nakamura, R., Soler, M.R., Sun, J., Burns, S., Lenschow, D.H., 2001. Shallow drainage flows. *Boundary Layer Meteorol.* 101, 243–260.
- Malhi, Y., Baldocchi, D.D., Jarvis, P.G., 1999. The carbon balance of tropical, temperate and boreal forests. *Plant Cell Environ.* 22, 715–740.
- Massman, W.J., Lee, X., 2002. Eddy covariance flux corrections and uncertainties in long-term studies of carbon and energy exchanges. *Agric. For. Meteorol.* 113, 121–144.
- Miller, S.D., Goulden, M.L., Menton, M.C., da Rocha, H.R., Freitas, H.C., Silva e Figueira, A.M., Dias de Sousa, C.A., 2003. Tower- and biometry-based measurements of tropical forest carbon balance. *Ecol. Appl.*, (in press).
- Moore, K.E., Fitzjarrald, D.R., Sakai, R.K., Goulden, M.L., Munger, J.W., Wofsy, S.C., 1996. Seasonal variation in radiative and turbulent exchange at a deciduous forest in Central Massachusetts. *J. Appl. Met.* 35, 122–134.
- Pattey, E., Strachan, I.B., Desjardins, R.L., Massheder, J., 2002. Measuring nighttime CO_2 flux over terrestrial ecosystems using eddy covariance and nocturnal boundary layer methods. *Agric. Forest Meteorol.* 113, 145–158.
- Raupach, M.R., Weng, W.S., Carruthers, D.J., Hunt, J.C.R., 1992. Temperature and humidity fields and fluxes over low hills. *Q.J.R. Meteorol. Soc.* 118, 191–225.

- Sakai, R.K., Fitzjarrald, D.R., Moore, K.E., 2001. Importance of low-frequency contributions to eddy fluxes observed over rough surfaces. *J. Appl. Met.* 40, 2178–2192.
- Savage, K.E., Davidson, E.A., 2001. Interannual variation of soil respiration in two New England forests. *Global Biogeochem. Cycles* 15, 337–350.
- Staebler, R.M., Fitzjarrald, D.R., Moore, K.E., Czikowsky, M.J., Acevedo, O.C., 2000. Topographic effects on flux measurements at Harvard Forest. In: *Proceedings of the 14th Symposium on Boundary Layers and Turbulence/9th Conference on Mountain Meteorology*, 7–11 August, 2000. Aspen, CO.
- Staebler, R.M., Fitzjarrald, D.R., Czikowsky, M.J., Sakai, R.K., 2001. Nocturnal CO₂ fluxes and understory drainage flows. *EOS Trans. AGU*, 82(47), Fall Meet. Suppl., Abstract B51A-0176
- Staebler, R.M., Fitzjarrald, D.R., Czikowsky, M.J., Sakai, R.K., 2002. The role of understory flows in forest carbon budgets. In: *Proceedings of the 15th Symposium on Boundary Layers and Turbulence*, 15–19 July, 2002. Wageningen, The Netherlands.
- Staebler, R.M., 2003. Forest subcanopy flows and micro-scale advection of carbon dioxide. PhD Dissertation, SUNY Albany.
- Sun, J., Desjardins, R., Mahrt, L., MacPherson, I., 1998. Transport of carbon dioxide, water vapor, and ozone by turbulence and local circulations. *J. Geophys. Res.* 103, 25873–25885.
- Wilson, K.B., Meyers, T.P., 2001. The spatial variability of energy and carbon dioxide fluxes at the floor of a deciduous forest. *Boundary Layer Meteorol.* 98, 443–473.
- Wofsy, S.C., Goulden, M.L., Munger, J.W., Fan, S.-M., Bakwin, P.S., Daube, B.C., Bassow, S.L., Bazzaz, F.A., 1993. Net exchange of CO₂ in a mid-latitude forest. *Science* 260, 1314–1317.
- Yi, C., Davis, K.J., Bakwin, P.S., Berger, B.W., Marr, L.C., 2000. Influence of advection on measurements of the net ecosystem-atmosphere exchange of CO₂ from a very tall tower. *J. Geophys. Res.* 105, 9991–9999.